A mathematical study of fractional order unsteady natural convective Casson fluid flow past an infinitely vertical plate with heat and mass transfer

Sapna Tyagi [1], Monika Jain [1*], Jagdev Singh[1]

[1] Department of Mathematics, JECRC University, Jaipur-303905, Rajasthan, India

tyagisapna1990@gmail.com, monikaj@gmail.com, jagdevsinghrathore@gmail.com

Abstract. Research on Casson fluid is very important due to its applicability in the progress of industrial and engineering industries. Here, a fractional order model of the Casson fluid over an oscillating plate in the presence of thermal radiation with constant wall temperature and concentration has been considered. The solution of this fractional model is obtained with the help of Laplace transform technique in terms of Wright function. The graphical analysis is also done by making several variations in parametric values including fractional parameter, mass Grashoff number, Prandtl number, velocity, temperature, concentration profiles etc.

1. Introduction

The physical characteristic of non-Newtonian fluid is always a barrier for researchers while solving the problems of non-Newtonian fluid. There is yet no comprehensive model that covers every aspect of a non-Newtonian fluid. Non-Newtonian fluid is widely used in the manufacturing and processing industries, thus researchers are constantly attempting to develop new models. One of the models is the Casson fluid model. In 1959, Casson [22] was the first to present the rheological data of pigment oil suspensions in printing ink.

Khalid et al. [1] studied the Casson fluid across an oscillating vertical plate for Unsteady boundary layer flow with constant wall temperature.

2010 *Mathematics Subject Classification.* 34A34, 26A33.

Key words and phrases. Casson fluid, fractional order, Wright function, Laplace transform.

*Corresponding Author.

Mahantesh et al. [4] studied the convective flow of Casson fluid across an oscillating plate using non-coaxial rotation and quadratic density fluctuation as its boundary conditions. Using variables without dimensions, the governing equations were first transformed into a non - dimensional form. Analytical solutions of the dimensionless momentum, heat, and mass equations were achieved using the Laplace transform method.

Using an exponentially permeable decreasing sheet, Nadeem et al. [25] investigated the boundary layer MHD flow of Casson fluid. The Adomian decomposition method was employed to arrive at the analytical answer to the problem. The velocity distributions resulting from a number of fascinating parameters were displayed and investigated.

The role of the magnetic flux on the three-dimensional Casson fluid flow over the boundary layer of a stretching porous sheet was taken into account in the study by Nadeem et al., [26] . It was discovered that the magnetic field, Casson fluid parameter, and porosity parameter all reduced the velocity profiles in the x and y directions.

The effects of chemical processes and heat generation of MHD convection Casson fluid flow model in a porous media using a revolving vertical plate is provided in the study done by Khan et al. [5].

The unstable MHD free convection flow of Casson fluid through a porous medium past a vertical plate that was moving exponentially was explored by Mohan et al.[24] in the presence of thermal radiation, chemical interaction, and a heat source or sink. They discovered that the velocity profiles decrease when the heat flow, magnetic field parameter, prandtl number, heat source, and Casson parameter increase in value.

Deka [3] has conducted studies of an unstable MHD casson fluid in nanopores with heat transfer through an accelerating vertical plate. It has been discovered that the Casson parameter increases skin friction and fluid velocity. Along with the casson parameter, the surface shear stress also rises.

It is assumed that the Casson fluid, a shear-thinning fluid, has infinite viscosity at zero rate of shear, zero viscosity at infinite rate of shear, and a yield stress below which no flow occurs. A fluid behaves like a solid when it is under conditions where the yield stress is greater than the shear stress. When the applied yield stress is greater than the applied shear stress, the fluid starts to flow. Casson fluid can take the form of things like honey, soup, chocolate, tomato sauce, jelly, blood, sludge, fused polymers, etc. These fluid models have been shown to have important uses in the biomechanics, textile, cosmetic, polymer processing, and pharmaceutical industries.

The Casson fluid flow across an oscillating plate with chemical reaction and sliding phenomenon was expressed by Saqib et al. [16]. The investigation concentrated on the mass and heat transport processes. The Laplace transform method was used to analyse the mathematical model once it had been transformed into dimensionless form. The profiles of velocity, temperature, and concentration were plotted.

Fractional derivatives have recently piqued the interest of many scholars due to the extensive coverage of derivatives and integrals of non-integer order. A variety of physical phenomena or natural circumstances have been studied with the help of fractional calculus, together with the rheological properties of winding polymers, traffic modelling, electric circuits, signal and image processing, electrical networks, stochastic processes and bioengineering.

Imran et al. [18] used two distinct fractional derivatives known as Caputo and Caputo-Fabrizio to study the convection flow of Newtonian fluid.The solutions to the concentration , temperature and velocity profiles were discovered by using the Laplace transform approach. The results were graphically depicted to compare and contrast the two fractional derivatives.

Also, the Caputo time-fractional derivatives are used by Imran et al. [19] to formulate fluid flows with Newtonian heating and arbitrary velocities.It was possible to obtain the dimensionless form of the governing equations by using the specified dimensionless variables. Using the Laplace transform approach, the dimensionless equations were solved.

Numerous scholars have noted the impact of fractional parameters on temperature and velocity characteristics. The computational analysis of fractional diffusion equations occurring in oil pollution has been done by Singh et al., [12].Research by Khan et al.,[11]gives the effect of fractional Caputo time derivatives of general Cassonian fluids with oscillating boundary conditions.

Ali et al. [9] employed the Caputo fractional derivative to examine the blood flow in a horizontal cylinder that was simulated by a Casson fluid. Magnetic particles were present in the fluid flow that was being driven by an oscillating pressure gradient. With the use of finite Hankel and Laplace transformations, the effects of magnetodynamics on Casson's fluids have been investigated and described.

The researchers observed that the fractional order fluid model performs noticeably differently from the conventional model. Several recent important analytical investigations on fluid problems can be found in preceding study [7], [8], [24], and [24].

Atangana-Baleanu and Caputo-Fabrizio are two fractional derivatives that are compared in Sheikh et al. comparative analysis for the convection of Casson's liquid across an infinite vertical flat plate, together with heat and mass transfer[20].

The researchers discovered that for a given unit of time, the velocities calculated using the Caputo-Fabrizio and Atangana-Baleanu operators are the same. Exact solutions for both situations were discovered using the Laplace transform methodology, and the outcomes were compared graphically and in tabular form.On the other hand, when time is less than unity, variance occurs and further differences increase as time increases.
For more definitions and results about the fractional operators, the reader can referes to [5], [13], [14].

2. Mathematical formulation of the problem

The present study takes into account the in compressible Casson fluid flow past an infinitely vertical plate in a free convection flow that is unsteady. Here, the flow range is $y > 0$, and y is the plate's coordinate normal.Primarily, at a time $\tau = 0$, the fluid and the plate are both at rest with a uniform surface concentration of C_∞^* and temperature T_∞^*. The plate begins to accelerate in its plane at time $\tau > 0$ according to a velocity $A\tau$, where unvarying A represents the plate's acceleration. Both the concentration and plate temperature are increased simultaneously to $T_\infty^*$and C_∞^* respectively, and then kept constant. The spatial variable y and the time variable t affect the velocity and temperature.

Following the use of the Boussinesq approximation and unidirectional flow, the momentum, energy, and concentration equations acquire the following forms.

$$\rho\frac{\partial \mathrm{u}^*}{\partial \tau^*} = \mu\left(1+\frac{1}{\beta}\right)\frac{\partial^2 \mathrm{u}^*}{\partial \mathrm{y}^{*2}} + \rho \mathrm{g}\gamma\left(\mathrm{T}^* - \mathrm{T}_\infty^*\right) + \rho \mathrm{g}\beta'\left(\mathrm{C}^* - \mathrm{C}_\infty^*\right), \tag{2.1}$$

$$\rho \mathrm{c_p}\frac{\partial \mathrm{T}^*}{\partial \tau^*} = \mathrm{k}\frac{\partial^2 \mathrm{T}^*}{\partial \mathrm{y}^{*2}} - \frac{\partial \mathrm{q_r^*}}{\partial \mathrm{y}^*}, \tag{2.2}$$

$$\frac{\partial \mathrm{C}^*}{\partial \tau^*} = \frac{1}{\mathrm{S_c}}\frac{\partial^2 \mathrm{C}^*}{\partial \mathrm{y}^{*2}}. \tag{2.3}$$

Here, β refers Casson parameter, u^* represent fluid in the y-direction, and time variable is denoted by τ^*. The fluid temperature near the plate is T^*, while T_∞^* refers plate's temperature. ρ denotes fluid density,μ is dynamic viscosity, Y refers to coefficients of the thermal expansion, q_r^* present radiative heat flux, c_p is the heat constant pressure, S_c is Schmidt number, k denotes thermal conductivity.

C^* is the concentration of the fluid near the plate, while C^*_∞ refers concentration of the plate associated with initial and boundary conditions:

$$\left.\begin{array}{c} u^*\left(y^*,0\right)=0, u^*\left(0,\tau^*\right)=\mathrm{F}\tau^{**}; u^*\left(\infty,\tau^*\right)=0 \\ \mathrm{T}^*\left(\mathrm{y}^*,0\right)=\mathrm{T}^*_\infty, \mathrm{T}^*\left(0,\tau^*\right)=\mathrm{T}^*_\mathrm{w}, \mathrm{T}^*\left(\infty,\tau^*\right)=\mathrm{T}^*_\infty \\ \mathrm{C}^*\left(\mathrm{y}^*,0\right)=\mathrm{C}^*_\infty, \mathrm{C}^*\left(0,\tau^*\right)=\mathrm{C}^*_\mathrm{w}, \mathrm{C}^*\left(\infty,\tau^*\right)=\mathrm{C}^*_\infty \end{array}\right\} \tag{2.4}$$

q^*_r is the radiative heat flux in equation (2.2). When q^*_r is differentiated in terms of y using Rosseland's approximation [2],[10],[27],[28], equation (2.2) becomes:

$$\rho c_p \frac{\partial T^*}{\partial \tau^*} = k\frac{\partial^2 T^*}{\partial y^{*2}} - \left(-\frac{16\sigma {T^*_\infty}^3}{3k^*}\right)\frac{\partial^2 T^*}{\partial y^{*2}}. \tag{2.5}$$

3. Problem Solution

The fundamental dimensional equations (2.1), (2.3), and (2.5) are changed into dimensionless equations. The solutions are then derived by employing the Laplace transform approach.
By employing appropriate dimensionless variables,

$$\mathrm{u}=\frac{\mathrm{u}^*}{(\vartheta\mathrm{A})^{\frac{1}{3}}}, \mathrm{t}=\frac{\tau^*(\mathrm{A})^{\frac{2}{3}}}{(\vartheta)^{\frac{1}{3}}}, \mathrm{y}=\frac{\mathrm{y}^*(\mathrm{A})^{\frac{1}{3}}}{(\vartheta)^{\frac{2}{3}}}, \mathrm{T}=\frac{\mathrm{T}^*-\mathrm{T}^*_\infty}{\mathrm{T}^*_\mathrm{w}-\mathrm{T}^*_\infty}\, and\, \mathrm{C}=\frac{\mathrm{C}^*-\mathrm{C}^*_\infty}{\mathrm{C}^*_\mathrm{w}-\mathrm{C}^*_\infty}. \tag{3.1}$$

The governing momentum (2.1), concentration (2.3) and energy (2.5) equations in the dimensionless form in view of (3.1) are

$$\frac{\partial \mathrm{u}}{\partial \mathrm{t}} = \left(1+\frac{1}{\beta}\right)\frac{\partial^2 \mathrm{u}}{\partial \mathrm{y}^2} + \mathrm{GrT} + \mathrm{GmC}, \tag{3.2}$$

$$\mathrm{S_c}\frac{\partial \mathrm{C}}{\partial \mathrm{t}} = \frac{\partial^2 \mathrm{C}}{\partial \mathrm{y}^2}, \tag{3.3}$$

$$\frac{\partial \mathrm{T}}{\partial \mathrm{t}} = \left(\frac{1+\mathrm{N}}{\mathrm{Pr}}\right)\frac{\partial^2 \mathrm{T}}{\partial \mathrm{y}^2}. \tag{3.4}$$

Also the boundary conditions (2.4) takes the form

$$\left.\begin{array}{c} \mathrm{u}\left(\mathrm{y},0\right)=0, \mathrm{u}\left(0,\tau\right)=\mathrm{t}; \mathrm{u}\left(\infty,\tau\right)=0 \\ \mathrm{T}\left(\mathrm{y},0\right)=0, \mathrm{T}\left(0,\tau\right)=1, \mathrm{T}\left(\infty,\tau\right)=0 \\ \mathrm{C}\left(\mathrm{y},0\right)=0, \mathrm{C}\left(0,\tau\right)=1, \mathrm{C}\left(\infty,\tau\right)=0. \end{array}\right\} \tag{3.5}$$

Next, equations (3.2), (3.3), and (3.4) are defined in terms of Caputo fractional derivatives as:

$$\mathrm{D}^\alpha_\mathrm{t}\mathrm{u} = \left(1+\frac{1}{\beta}\right)\frac{\partial^2 \mathrm{u}}{\partial \mathrm{y}^2} + \mathrm{GrT} + \mathrm{GmC}, \tag{3.6}$$

$$\mathrm{S_c D_t^\alpha C} = \frac{\partial^2 \mathrm{C}}{\partial \mathrm{y}^2}, \tag{3.7}$$

$$\left(\frac{\mathrm{Pr}}{1+\mathrm{N}}\right)\mathrm{D_t^\alpha T} = \frac{\partial^2 \mathrm{T}}{\partial \mathrm{y}^2}, \tag{3.8}$$

where D denotes the differential operator, the fractional operator is α, whereas Gr, N, Pr and Gm are the thermal Grashof number, radiation and Prandtl number and mass Grashof number respectively.

4. Laplace Transform Technique

Unsteady differential equations are frequently solved using the Laplace transform, an integral transform technique. The second order differential equations for the partial differential equations (3.2), (3.3), and (3.4)are generated on using the Laplace transform technique.

$$\left(1+\frac{1}{\beta}\right)\frac{\mathrm{d}^2\bar{u}}{\mathrm{dy}^2} - \mathrm{s}^\alpha \bar{u}\left(\mathrm{y,s}\right) + \mathrm{Gr}\bar{T} + \mathrm{Gm}\bar{C} = 0, \tag{4.1}$$

$$\frac{\mathrm{d}^2\bar{C}}{\mathrm{dy}^2} - \mathrm{s}^\alpha \mathrm{S_c}\bar{C}\left(\mathrm{y,s}\right) = 0, \tag{4.2}$$

$$\frac{\mathrm{d}^2\bar{T}}{\mathrm{dy}^2} - \left(\frac{\mathrm{Pr}}{1+\mathrm{N}}\right)\mathrm{s}^\alpha \bar{T}\left(\mathrm{y,s}\right) = 0. \tag{4.3}$$

Eq. (4.1), (4.2) and (4.3) are then solved by using the undetermined coefficient method and the solutions are presented as

$$\bar{u}\left(\mathrm{y,s}\right) = \frac{1}{\mathrm{s}^2}\mathrm{e}^{-\mathrm{y}\sqrt{\frac{\mathrm{s}^\alpha}{\mathrm{z}}}} + \frac{\mathrm{Gr_0}}{\mathrm{s}^{\alpha+1}}\mathrm{e}^{-\mathrm{y}\sqrt{\frac{\mathrm{s}^\alpha}{\mathrm{z}}}} + \frac{\mathrm{Gm_0}}{\mathrm{s}^{\alpha+1}}\mathrm{e}^{-\mathrm{y}\sqrt{\frac{\mathrm{s}^\alpha}{\mathrm{z}}}} - \frac{\mathrm{Gr_0}}{\mathrm{s}^{\alpha+1}}\mathrm{e}^{-\mathrm{y}\sqrt{\mathrm{as}^\alpha}} - \frac{\mathrm{Gm_0}}{\mathrm{s}^{\alpha+1}}\mathrm{e}^{-\mathrm{y}\sqrt{\mathrm{S_c s}^\alpha}}, \tag{4.4}$$

$$\bar{T}\left(\mathrm{y,s}\right) = \frac{1}{\mathrm{s}}\mathrm{e}^{-\mathrm{y}\sqrt{\mathrm{as}^\alpha}}, \tag{4.5}$$

$$\bar{C}\left(\mathrm{y,s}\right) = \frac{1}{\mathrm{s}}\mathrm{e}^{-\mathrm{y}\sqrt{\mathrm{S_c s}^\alpha}}, \tag{4.6}$$

where $\mathrm{z} = \left(1+\frac{1}{\beta}\right), \mathrm{a} = \left(\frac{\mathrm{Pr}}{1+\mathrm{N}}\right), \mathrm{Gr_0} = \frac{\mathrm{Gr}}{(\mathrm{az}-1)}$ and $\mathrm{Gm_0} = \frac{\mathrm{Gm}}{(\mathrm{S_c z}-1)}$. The final solution to the problem is provided by taking inverse Laplace of equations (4.4), (4.5), and (4.6).

$$\begin{aligned}\mathrm{u}\left(\mathrm{y,t}\right) = {} & \mathrm{t}\varphi\left(2, -\tfrac{\alpha}{2}; -\mathrm{y}\sqrt{\tfrac{\mathrm{s}^\alpha}{\mathrm{z}}}\mathrm{t}^{-\frac{\alpha}{2}}\right) + \tfrac{\mathrm{Gr_0}}{\Gamma(\alpha)}\mathrm{t}^{\alpha-1}\varphi\left(1, -\tfrac{\alpha}{2}; -\mathrm{y}\sqrt{\tfrac{\mathrm{s}^\alpha}{\mathrm{z}}}\mathrm{t}^{-\frac{\alpha}{2}}\right) \\ & + \tfrac{\mathrm{Gm_0}}{\Gamma(\alpha)}\mathrm{t}^{\alpha-1}\varphi\left(1, -\tfrac{\alpha}{2}; -\mathrm{y}\sqrt{\tfrac{\mathrm{s}^\alpha}{\mathrm{z}}}\mathrm{t}^{-\frac{\alpha}{2}}\right) - \tfrac{\mathrm{Gr_0}}{\Gamma(\alpha)}\mathrm{t}^{\alpha-1}\varphi\left(1, -\tfrac{\alpha}{2}; -\mathrm{y}\sqrt{\mathrm{a}}\mathrm{t}^{-\frac{\alpha}{2}}\right) \\ & - \tfrac{\mathrm{Gm_0}}{\Gamma(\alpha)}\mathrm{t}^{\alpha-1}\varphi\left(1, -\tfrac{\alpha}{2}; -\mathrm{y}\sqrt{\mathrm{S_c}}\mathrm{t}^{-\frac{\alpha}{2}}\right),\end{aligned} \tag{4.7}$$

$$\mathrm{C}\left(\mathrm{y},\mathrm{t}\right)=\varphi\left(1,-\frac{\alpha}{2};-\mathrm{y}\sqrt{\mathrm{S_c}}\mathrm{t}^{-\frac{\alpha}{2}}\right), \tag{4.8}$$

$$\mathrm{T}\left(\mathrm{y},\mathrm{t}\right)=\varphi\left(1,-\frac{\alpha}{2};-\mathrm{y}\sqrt{\mathrm{a}}\mathrm{t}^{-\frac{\alpha}{2}}\right), \tag{4.9}$$

where $\varphi\left(a,-\varrho;\zeta\right)=\sum\limits_{n=0}^{\infty}\frac{(\zeta)^n}{n!\Gamma(a-n\varrho)}$ is the Wright function.
Equations (4.7)–(4.9) are bounded by boundary conditions as in (3.5).

5. Result and Discussion

For the free convection flow of a generalised fractional Casson fluid over an accelerating plate, equations (4.4), (4.5), and (4.6) show the closed form. The graphs are generated with varied values of embedded parameters to study how different parameters affect the profiles of velocity, concentration, and temperature. The purpose of the graphs 1-3 is to investigate the impact of the fractional parameter, Prandtl number Pr, and N radiation on temperature profiles with different values.Figures 4–7 display the velocity profile graphs, which were plotted with various fractional parameters, Casson fluid parameters, mass Grashoff number Gm, and time t. In the meantime, Figure 8 shows validation of current solutions.

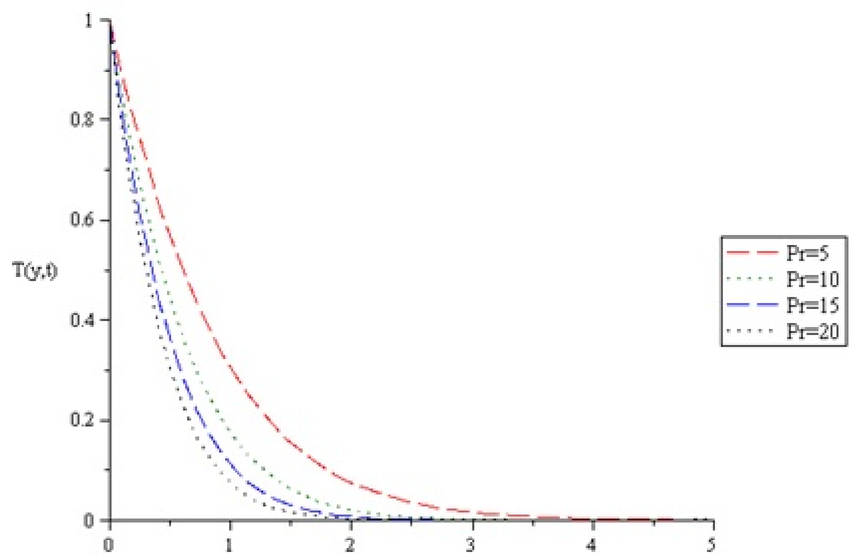

Fig1. Temperature profile with different Pr

The Prandtl number's impact on the temperature distribution is shown in Figure 1. The graph shows that as the value of Pr rises, the temperature profile rapidly falls. The thermal and momentum diffusivity relationship is defined by Prandtl number. Further, the thermal boundary layer thickness is more than the thickness of the momentum boundary layer when Pr , the Prandtl number is small because the fluid travels more slowly than heat transfer. Therefore, for higher Pr fluids, heat can flow from the sheet more quickly. However, a bigger Prandtl number might result in a thinner thermal boundary layer, which would then result in a weaker thermal force for transport and a lower temperature profile.

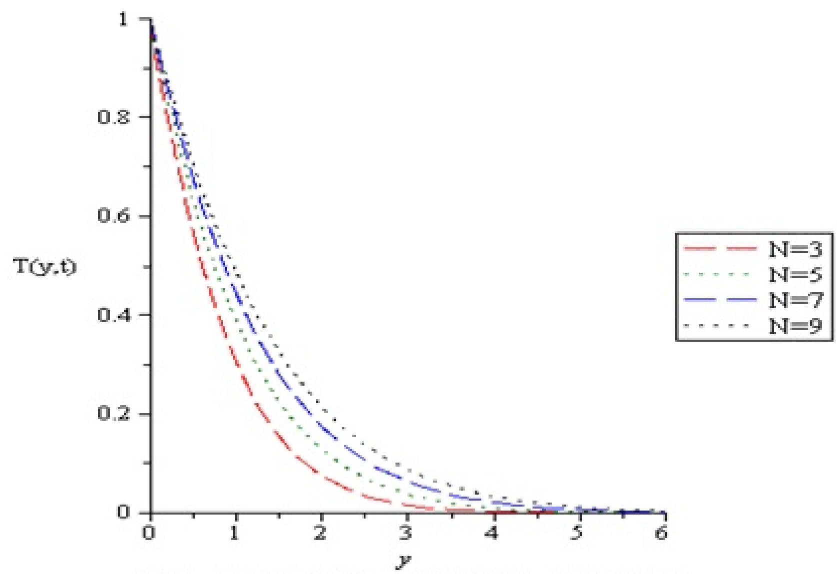

Fig2. Temperature profile with different N

Figure 2 displays the temperature profile of thermal radiation for constant values of Pr and t and various values of N. It is evident that a rise in temperature causes a rise in thermal radiation. The fluid temperature rises as a result of the growing radiation parameter's rising temperatures absorption.

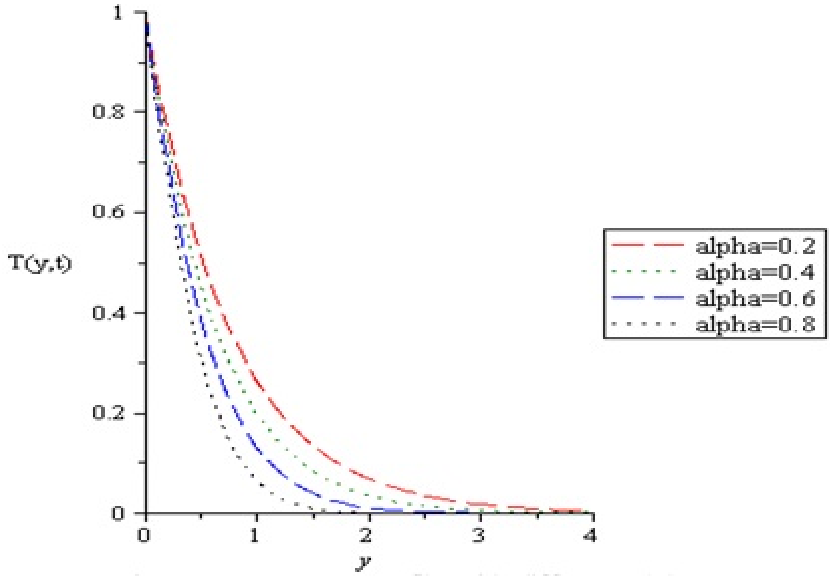

Fig3. Temperature profile with different alpha

Figure 3 illustrates the effect of fractional parameters on temperature. As shown in the figure, the temperature increases monotonically as falls. The outcome here can be helpful for a few real-world issues. By using the computed theoretical results and a suitable fractional mathematical model, the expected outcome and the range for an experimental design are assessed.

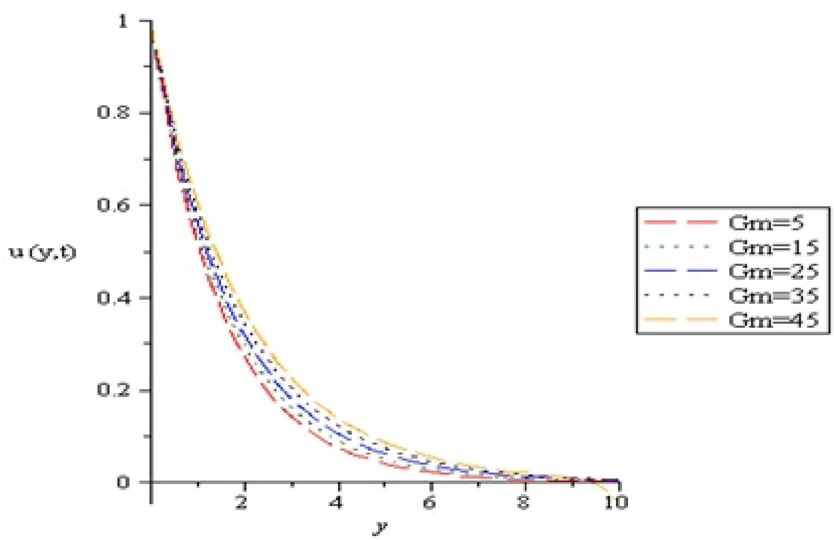

Fig4. Velocity profile with different Gm

The impact of the Grashoff number Gm on the velocity profile is depicted in Figure 4. It is possible to claim that when the value of Gm has been increased, the velocity value also goes up gradually.

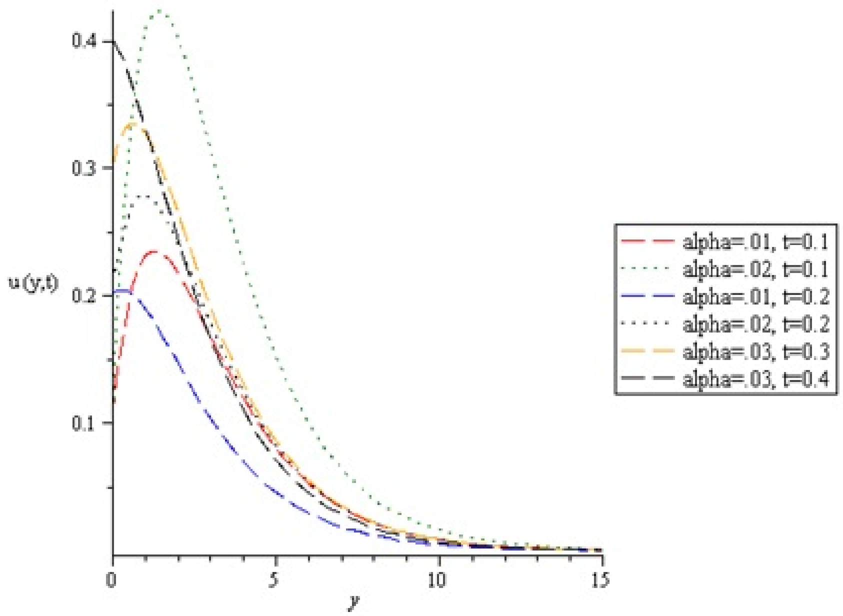

Fig5. Velocity profile with different t & alpha

Figure 5 effects of time and alpha toward the velocity. The velocity increases dramatically in figure 5.

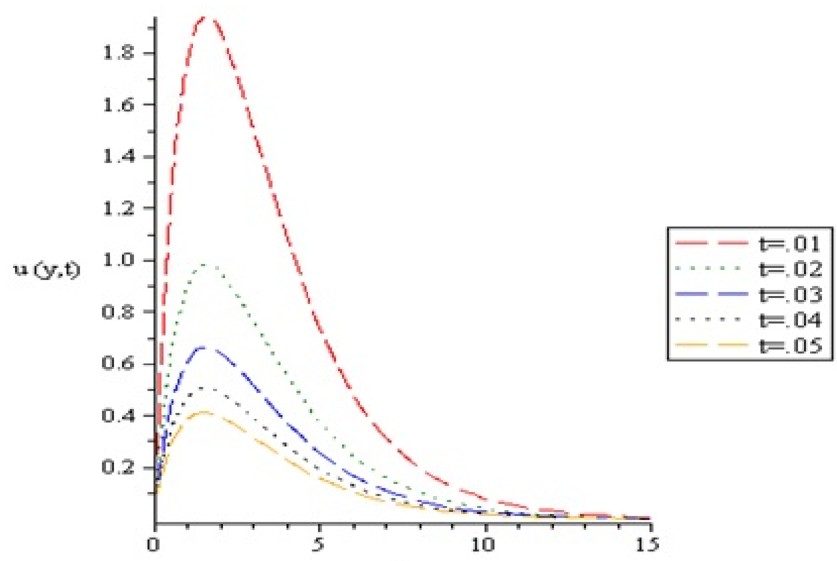

Fig 6. Velocity profile with different t

The impact of time t on velocity profiles is shown in Figure 6. The velocity declines but at a different rate as the value of t rises. The velocity decreases sharply in Figure 6. This tendency can be explained by the graphs' trend which indicates that as t increases, the energy produced by the fluid flow will eventually fall as well.

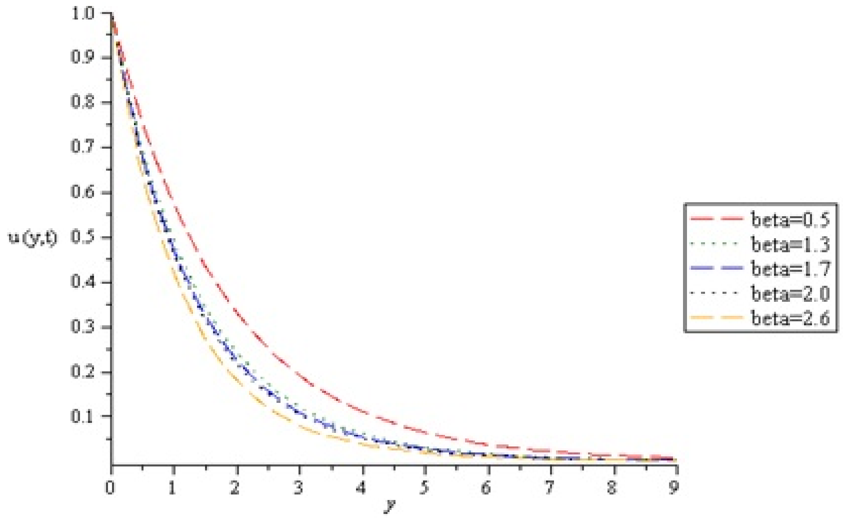

Fig 7. Velocity profile with different beta

The impact of the velocity profile by the Casson parameter is depicted in Figure 7. The velocity initially suffers a falling tendency before progressively increasing.

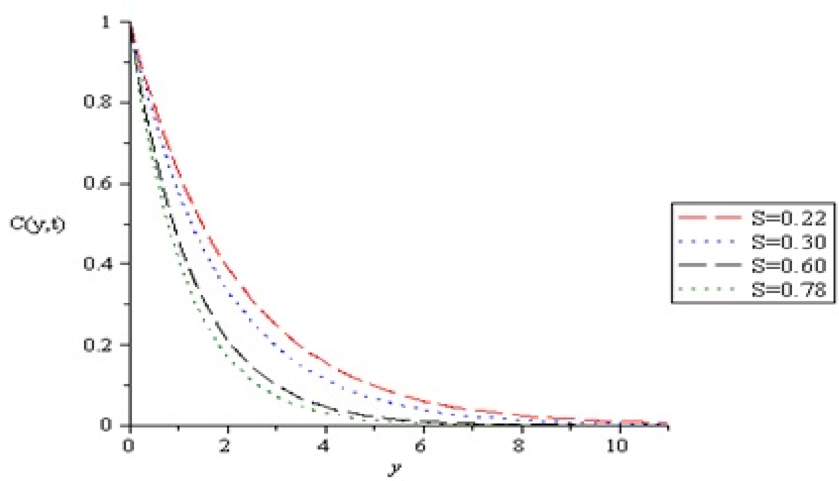

Fig 8. Concentration profile with different Schmidt number (S)

Schmidt number S's impact on the concentration profile may be seen in Figure 8.The value of concentration decrease progressively as the value rise up.

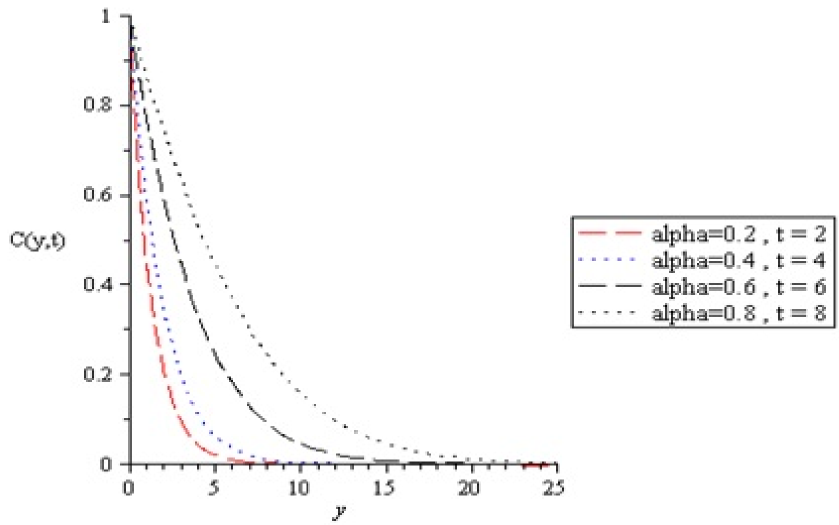

Fig 9. Concentration profile with different alpha and t

Figure 9 shows the effect of t and alpha on the concentration profile. As the value of t and alpha increases, the value of concentration raised steadily.

6. Conclusion

An accelerating plate's free convection flow of fractional order Casson fluid flow has been investigated in the present study. The solutions for velocity and temperature were obtained using the Laplace transform approach.The impact of several parameters on fluid flow, including the Casson fluid parameter, fractional parameter, time, Schmidt number (S), thermal radiation (N), and Prandtl number, is explored. Additionally, it is considered that the obtained results are reliable and provide a new points of view on Casson fluid flow.

References

[1] A. Khalid, I .Khan and S. Shafie, "Unsteady boundary layer flow of a casson fluid past an oscillating vertical plate with constant wall temperature." Malaysian Journal of Fundamental and Applied Science 11, no.1, 28-32(2015).

[2] A.B.M. Raju., P.R. Chandra, B. Malikarjuna and C.S.K. Raju, "Radiation absorption and Soret effects on MHD conducting fluid flow past an exponentially accelerated vertical plate." South East Asian J. Math . Math. Sci., vol. 2'1, no. 1, 1-9 (2020).

[3] A.K. Deka, "In the presence of thermal radiation through porous medium unsteady MHD casson fluid flow past an accelerated vertical plate." International Journal of Statistics and Applied Mathematics 5, no. 4, 213-228 (2020).

[4] B. Mahanthesh, T. Brizlyn, S. Shehzad and B. J. Gireesha, "Nonlinear Thermo-Solution Convective Flow of Casson Fluid over an Oscillating Plate Due to Non-Coaxial Rotation with Quadratic Density Fluctuation Exact Solutions." Multidiscipline Modeling in Materials and Structures 15, 818–8424 (2018).

[5] C. Li, D. Qian and Y. Chen, "On Riemann- Liouville and Caputo Derivative.", Discrete Dynamics in Nature and Society, vol.2011, Article Id 562494, (2011).

[6] D. Khan, A. Khan, I. Khan, F. Ali, F. ul. Karim and I. Tlili, "Effects of relative magnetic field, chemical reaction, heat generation and newtonian heating on convection flow of casson fluid over a moving vertical plate embedded in a porous medium." Scientific Reports 9, no. 1, 1–18(2019).

[7] E.K. Ghiasi and R. Saleh, "Analytical and numerical solutions to the 2d sakiadis flow of casson fluid with cross diffusion, inclined magnetic force, viscous dissipation and thermal radiation based on buongiorno's mathematical model." CFD Letters 11, no. 1, 40–54(2019).

[8] E.K. Mahmoud, "Analytical solution of modified bingham fluid flow through parallel plates channel subjected to forchheimer medium and hall current using linearized differential transformation method." Journal of Advanced Research in Numerical Heat Transfer 4, no. 1, 14–31(2021).

[9] F. Ali, N.A. Sheikh, I. Khan and M. Saqib, "Magnetic field effect on blood flow of Casson fluid in axisymmetric cylindrical tube: A fractional model." Journal of Magnetism and Magnetic Materials 423, 327-336 (2017).

[10] F.S. Ibrahim, A.M. Elaiw and A.A. Bakar, "Effects of the chemical reaction and radition absorption on the unsteady MHD free convection flow past a semi infinite vertical permeable moving plate with heat source and suction." Commun. Nonlinear Sci. Numer. Simul., vol. 13, no. 6, 1056-1066 (2008).

[11] I. Khan, N.A.Shah and D.Vieru, "Unsteady flow of generalized Casson fluid with fractional derivative due to an infinite plate." The European Physical Journal Plus 131, no. 6, 1-12(2016).

[12] J. Singh, A.M. Alshehri, S. M. Momaniand S.B. Hadid, " Computational Analysis of Fractional Diffusion Equations Occurring in Oil Pollution." Mathematics, 10, 20 (2022).

[13] J. Singh, B. Ganbari, D. Kumar and D. Baleanu, "Analysis of fractional model of guava for biological pest control with memory effect." Journal of Advanced Research, 32, 99-108 (2021).

[14] J. Singh, D. Kumar and D. Baleanu, "A new analysis of fractional fish farm model associated with Mittag-Leffler type kernel." International Journal of Biomathematics, vol 13, no. 2(2020).

[15] M. A. Qushairi, N.A. Jaafar, S. Shafie, Z. Ismail and M. Qasim, "Theoretical study on rotating casson fluid in moving channel disk." In Journal of Physics: Conference Series, vol. 1366, no. 1, p. 012039. IOP Publishing, (2019).

[16] M. Saqib, F. Ali, I. Khan and N. A. Sheikh, "Heat and mass transfer phenomena in the flow of Casson fluid over an infinite oscillating plate in the presence of first-order chemical reaction and slip effect.' Neural Computing and Applications 30, no.7, 2159-2172(2018).

[17] M.A. Imran, M. Aleem, M.B. Riaz, R.Ali and I. Khan, "A comprehensive report on convective flow of fractional (ABC) and (CF) MHD viscous fluid subject to generalized boundary conditions." Chaos, Solutions & Fractals, 118, 274-289(2019).

[18] M.A. Imran, N. A.Shah, I. Khan, and M. Aleem, "Applications of non-integer Caputo time fractional derivatives to natural convection flow subject to arbitrary velocity and Newtonian heating." Neural Computing and Applications 30, no. 5, 1589-1599(2018).

[19] M.A. Imran, S. Sarwar, M. Abdullah and I. Khan, "An analysis of the semi-analytic solutions of a viscous fluid with old and new definitions of fractional derivatives." Chinese journal of physics 56, no. 5, 1853-1871(2018).

[20] M.G. Reddy, P.V. Kumari and P. Padma, "Effects of thermal radiation on MHD Casson fluid over a cylinder." J. Nanofluids, vol. 7, 428-438(2018).

[21] N. A. Sheikh, F. Ali, M. Saqib, I. Khan A.S. Alshomrani and M. S Alghamdi, "Comparison and analysis of the atangana–baleanu and caputo–fabrizio fractional derivatives for generalized casson fluid model with heat generation and chemical reaction." Results in Physics 7, 789–800(2017).

[22] N. Casson, "A flow equation for pigment –oil-suspensions of the printing ink type." Rhealogy of Disperse systems (1959).

[23] N. S. Wahid, M. E.H. Hafidzuddin, N. Md. Arifin, M. Turkyilmazoglu and N. A. Abd Rahmin, "Magnetohydrodynamic (MHD) slip darcy flow of viscoelastic fluid over a stretching sheet and heat transfer with thermal radiation and viscous dissipation." CFD Letters 12, no. 1 (2020).

[24] S.Mohan, G.V. Reddy and S. Balakrishna,"An unsteady MHD free convection flow of casson fluid past an exponentially accelerated infinite vertical plate through porous medium in the presence of the thermal radiation, chemical reaction and heat source or sink." International journal of engineering and techniques 4, no. 4, 16-27(2018).

[25] S. Nadeem, R. Ul Haq and C. Lee, "MHD flow of a Casson fluid over an exponentially shrinking sheet." Scientia Iranica 19, no. 6, 1550-1553(2012).

[26] S. Nadeem, R. Ul Haq, N.S. and Z. H. Khan, "MHD three-dimensional Casson fluid flow past a porous linearly stretching sheet." Alexandria Engineering Journal 52, no. 4, 577–882(2013).

[27] S. Pramanik, "Casson fluid flow and heat transfer past exponentially porous stretching surface in presence of thermal radiation." Ain Shams Eng. J., Vol. 5, no. 1, 205-212 (2014).

[28] S.R.Mohan,"Dufour and radiation absorption effects on unsteady MHD free convection casson fluid flow past an exponentially infinite vertical plate through porous medium." Vol. 6, no. 2, 485-512(2019).

[29] V.P. Dubey, J. Singh, A.M. Alshehri and S. Dubey, "Analysis of local fractional coupled Helmholtz and coupled Burgers' equations in fractal media." AIMS Mathematics, 7,5, 8080-8111 (2022).